



Synthesis, biological evaluation and SAR study of novel pyrazole analogues as inhibitors of *Mycobacterium tuberculosis*

Daniele Castagnolo^a, Alessandro De Logu^b, Marco Radi^a, Beatrice Bechi^a, Fabrizio Manetti^a, Matteo Magnani^a, Sibilla Supino^a, Rita Meleddu^b, Lorenza Chisu^b, Maurizio Botta^{a,*}

^a Dipartimento Farmaco Chimico Tecnologico, Università degli Studi di Siena, Via Aldo Moro, 53100 Siena, Italy

^b Sezione di Microbiologia Medica, Dipartimento di Scienze e Tecnologie Biomediche, Università di Cagliari, Viale Sant'Ignazio 38, 09123 Cagliari, Italy

ARTICLE INFO

Article history:

Received 28 April 2008

Revised 31 July 2008

Accepted 4 August 2008

Available online 7 August 2008

Keywords:

Tuberculosis

5-Hydroxy-pyrazole

Pyrazolone

SAR study

ABSTRACT

As a continuation of our previous work that turned toward the identification of antimycobacterial compounds with innovative structures, two series of pyrazole derivatives were synthesized by parallel solution-phase synthesis and were assayed as inhibitors of *Mycobacterium tuberculosis* (MTB), which is the causative agent of tuberculosis. One of these compounds showed high activity against MTB (MIC = 4 µg/mL). The newly synthesized pyrazoles were also computationally investigated to analyze their fit properties to the pharmacophoric model for antitubercular compounds previously built by us and to refine structure–activity relationship analysis.

© 2008 Elsevier Ltd. All rights reserved.

1. Introduction

Tuberculosis (TB) is an airborne infectious disease caused by *Mycobacterium tuberculosis* (MTB) and represents one of the leading causes of death worldwide. The World Health Organization (WHO) estimated that in 2005, 8.8 million people fell ill with TB and 1.6 million of them died. The dangerous spread of TB is mainly due to its association with HIV infection and to the development of multidrug-resistant (MDR) strains of MTB.¹ Another most alarming aspect is the emergence of extensively drug-resistant TB (XDR-TB) in the last years²; it poses a serious threat to TB control, and confirms the urgent need to discover new structural classes of antimycobacterial compounds in order to develop agents to replace or supplement the established drugs.³

Recently, we reported successful results on the identification of new antimycobacterial compounds with innovative structures through a computational procedure for the generation, design, and screening of a ligand-based virtual library. A 5-hydroxy-pyrazole compound with general structure **A**, characterized by a MIC of 25 µg mL⁻¹, emerged as a hit candidate from virtual screening. Consequent optimization of the hit and synthesis of a library of derivatives led us to obtain pyrazoles **1–3** as interesting compounds with enhanced antimycobacterial activity, namely MIC of 6.25 µg mL⁻¹ for **1** and **2** and MIC of 12.5 µg mL⁻¹ for **3** (Fig. 1, Table 1).⁴ The major suggestion derived from the biological results

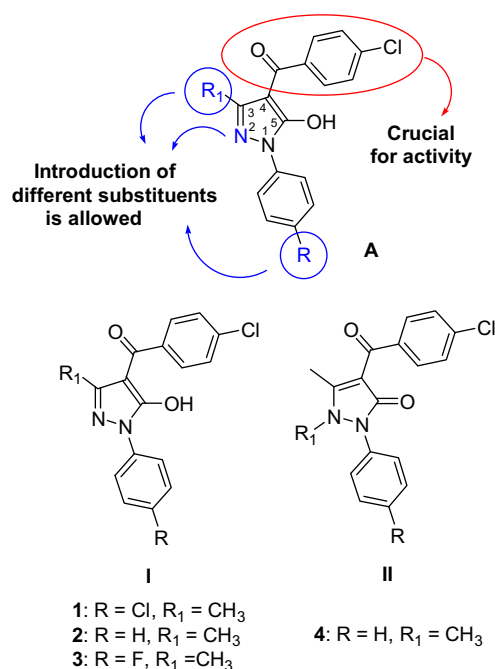


Fig. 1. Hit compounds **1–3** and previous structure–activity relationship considerations.

* Corresponding author. Tel.: +39 0577 234 306; fax: +39 0577 234 333.

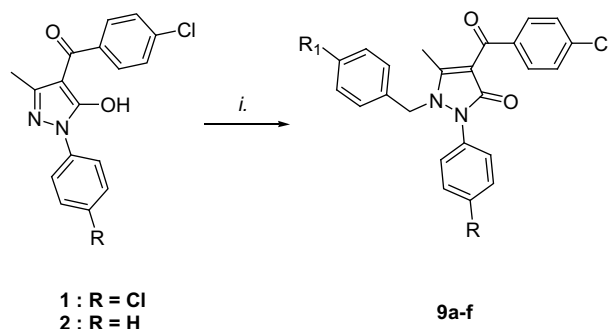
E-mail address: botta@unisi.it (M. Botta).

was that the *p*-chlorobenzoyl moiety at C4 of the pyrazole ring with general structure **A** was the fundamental for the activity. However, no investigations were carried out on the effects that the introduction of different substituents at N1, N2, and C3 of the pyrazole ring might produce on antimycobacterial activity. As a consequence, in an attempt to increase the fitting to the pharmacophoric model, and possibly to optimize the bind to the hypothetical receptor, we report here the synthesis, biological activity, and SAR study of two series (**I** and **II**) of second generation pyrazole/pyrazolones derivatives. Series **I**, constituted by analogues of compounds **1–3** (Fig. 1), was designed to investigate on the influence exerted on the activity by synthetic derivatizations at C3 and on the N1-phenyl ring, keeping the *p*-chlorobenzoyl moiety at C4 fixed, which was suggested to be crucial for the activity. On the other hand, series **II** was based on the structure of pyrazolone **4** previously synthesized by us although its activity toward MTB was $>100 \mu\text{g mL}^{-1}$. This series was based on the insertion of substituents at the N2 of the pyrazole ring, a position not investigated in previous antimycobacterial pyrazolone derivatives, while keeping a methyl group at C3 fixed. In detail, following what was reported in the literature about the importance of an additional aromatic group on the central pyrazole nucleus,⁵ different benzyl groups were chosen to be introduced at N2.

2. Chemistry

A series of analogues of **1–3** (series **I**) were synthesized in parallel using a Büchi Syncore synthesizer⁴ as illustrated in Scheme 1. β -Ketoesters **5a–d** were placed in 11 different reaction vessels, and reacted in parallel with five different phenylhydrazines **6a–e**. After the reactions were completed, *p*-toluenesulfonic acid polymer-bound scavenger was added to remove the excess of hydrazines, and the mixtures were filtered in parallel to afford compounds **7a–k**.⁶ They were obtained together with a small amount of their regioisomers, resulting from the attack of hydrazines first on ester moiety and then on ketone moiety. Separation of the two regioisomers was possible by fractionate crystallization from an appropriate solvent. Reaction of desired pyrazolones with *p*-chlorobenzoyl chloride using the Jensen method afforded pyrazoles **8a–k**.⁷ These compounds were obtained in high yield after simple filtration-recrystallization procedure from the crude mixtures.

On the other hand, based on the knowledge that pyrazolones bearing three aromatic groups resulted to be active toward a wide range of bacteria,⁵ a series of *N*-2-benzyl derivatives **9a–f** (series **II**) were then synthesized starting from leads **1** and **2**. The aim of this second series was to investigate the effects that large and aromatic groups at N2, such as a benzyl group, might have on the antimycobacterial activity. Pyrazoles **1** and **2** were placed in six different reaction vessels and reacted in parallel with different benzyl halides using a Büchi Syncore synthesizer affording pyrazolones



Scheme 2. Reagents and conditions: (i) Benzyl halide, NaH, DMF, NaI Syncore, 300 rpm.

9a–f.^{8,9} The N2-alkylated derivatives were formed as the only products under these reaction conditions. No traces of O-alkylated isomers were observed. NOE experiments confirmed that the alkylation proceeded only at N2¹⁰ (see Scheme 2).

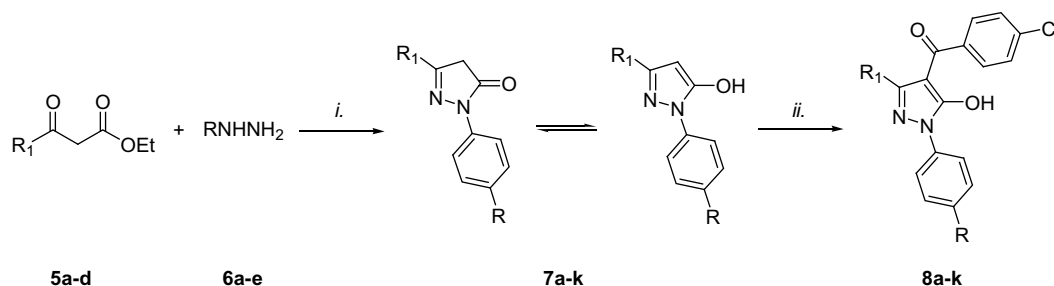
3. Results and discussion

Compounds were assayed for their inhibitory activity toward *M. tuberculosis* H37Rv (ATCC27294). The minimum inhibitory concentration ($\mu\text{g mL}^{-1}$) was determined for each compound (Table 1).

With regard to compounds **8a–k**, the introduction at C3 of groups different from the methyl substituent was in general detrimental for the activity, and never led to an improvement of the MIC values. The maintenance of a methyl group at C3, as in compounds **8g**, **8h**, and **8j**, resulted in medium or good activity values. Different hydrophobic substituents at *para* position of the N1-phenyl ring were tolerated. The pyrazole derivative **8g**, with the *p*-bromophenyl group at N1 position, showed to be very active (MIC = $4 \mu\text{g/mL}$), with a slightly higher activity than hit compounds **1** and **2**. Conversely, pyrazolone derivatives **9a–f**, keeping the methyl group at C3 fixed and bearing a 4-substituted-benzyl moiety at N2, resulted to be significantly more active than the methyl derivative **4**, even if they resulted to be less active than the pyrazole series.

4. Computational studies

The newly synthesized pyrazole derivatives were computationally investigated by means of the Catalyst software,¹¹ to analyze their fit properties to the pharmacophoric model for antitubercular compounds previously built.¹² Such a pharmacophore, consisting of two ring aromatic (RA1 and RA2), two hydrophobic (HY1 and HY2), and one hydrogen bond acceptor (HBA) features, was part of the virtual screening procedure which resulted in the discovery



Scheme 1. Reagents and conditions: (i) a—Syncore, 300 rpm, EtOH, reflux; b—*p*-toluenesulfonic acid polymer bound. (ii) *p*-Cl-C₆H₄COCl, Ca(OH)₂, Syncore, 300 rpm, dioxane, reflux.

of the hit compound **1**.⁴ As a result of the computational analysis, all the derivatives **8a–k** were found to map the pharmacophoric model with a very similar orientation, closely resembling that of compound **1** (Fig. 2). In detail, the pyrazole nucleus appeared to act as a scaffold to direct the phenyl moiety at N1 and the benzoyl moiety at C4 in the proper region of space, resulting in efficacious fitting of RA1 and RA2 features, respectively. The carbonyl group of each pyrazole derivative corresponded to the HBA feature of the pharmacophore. The methyl group at C3 was well accommodated into the hydrophobic region HY2, thus accounting for the good activity generally associated with the presence of a methyl substituent at this position. Introduction of bulkier hydrophobic substituents at C3, which still mapped but exceeded the HY2 function, resulted in compounds with decreased activity, suggesting that this region may be involved in a favorable hydrophobic interaction with the receptor counterpart, but unfavorable steric interactions could occur upon increasing the substituent's size. The halogen or alkyl substituents at the *para* position of the phenyl ring at N1 of derivatives **8d–k** well fitted the second hydrophobic region of the pharmacophoric model, namely HY1. However, it resulted that N1-phenyl-halogenated derivatives (namely **1**, **8f**, and **8g**) were more active than the corresponding N1-phenyl-alkyl compounds **8h–k**, keeping the substituent at C3 fixed. We might assume that the electronic nature of halogens on phenyl ring had a beneficial effect resulting in compounds with enhanced antimycobacterial activity. On the contrary, the presence in the same position of an electron-donating group, such as a methyl or an isopropyl group, resulted in a medium–high loss of activity. Among the different hydrophobic groups, the highest activity measured for **8g** indicated the bromine substituent as the most suitable one at this position.¹³ The complete lack of activity of compound **8f**, bearing a chlorine at the *para* position of the phenyl ring and a trifluoro substituent at C3 (able to fit the hydrophobic functions), was quite unexpected and could not be explained only with the spatial and functional information provided by the pharmacophoric model. Maybe the electron-withdrawing nature of trifluoro substituent produces an electronic destabilization of the pyrazole nucleus, resulting somehow in a loss of activity. On the basis of these speculations, it seems obvious that the electronic properties of the pyrazole derivatives play a crucial role in order to enhance the antimycobacterial activity.

On the other hand, the presence of a large benzyl substituent at N2 in compounds **9a–f** induced a rearrangement in the pharmacophoric model and a completely different mapping with respect to derivatives **8a–k** (Fig. 3). In more detail, the methyl group at C3 was still located in the hydrophobic region HY2, similar to compounds **8a–k**, while the phenyl and the benzyl moiety fitted the RA2 function well. The *para*-substituted phenyl ring at N1, which

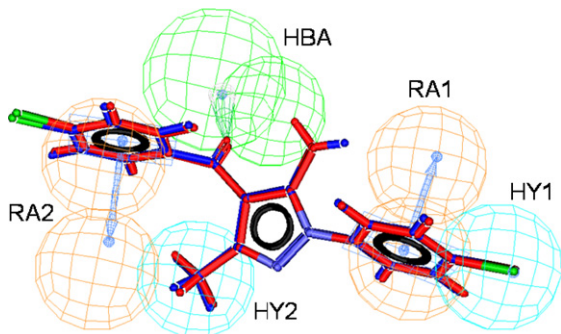


Fig. 2. Superposition of compound **1** (red) and **8g** (blue) onto the pharmacophoric model for antitubercular compounds. Features are color-coded (cyan: hydrophobic; orange: aromatic ring; green: hydrogen bond acceptor).

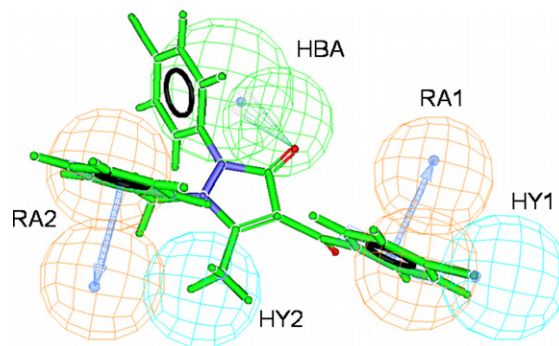


Fig. 3. Compound **9e** mapped to the pharmacophoric model. The color and orientation of features are the same as in Fig. 2.

emerged as important in modulating the activity in the previous set of compounds, was not relevant for interacting with the pharmacophoric elements. Finally, the HBA feature was mapped by the carbonyl group of the pyrazolone nucleus, a motif which was absent in derivatives **8a–k**. Remarkably, the substituents discriminating among compounds **9a–f** (namely, those at the *para* positions of the phenyl ring at N1 and the benzyl group at N2) were placed in a region of space where no pharmacophoric feature lies. This aspect impeded us to use the pharmacophoric model as a tool to rationalize the differences in activity detected for derivatives **9a–f**.

5. Experimental

Reagents were obtained from commercial suppliers and used without further purification. Dioxane was dried over Na/benzophenone prior to use. Anhydrous reactions were run under a positive pressure of dry N₂. Merck silica gel 60 was used for flash chromatography (23–400 mesh). ¹H NMR and ¹³C NMR spectra were measured at 200 MHz on a Bruker AC200F spectrometer and at 400 MHz on a Bruker Avance DPX400. Chemical shifts were reported relative to CDCl₃ at δ 7.24 ppm and to tetramethylsilane at δ 0.00 ppm. Büchi Syncore polyvap was used for parallel synthesis, filtration, and evaporation.

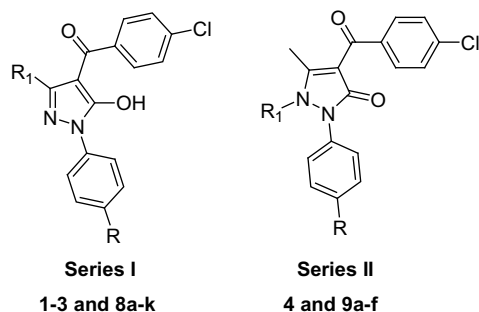
5.1. HPLC and MS analysis

The purity of compounds was assessed by reverse-phase liquid chromatography and a mass spectrometer (Agilent series 1100 LC/MSD) with a UV detector at λ = 254 nm and with an electrospray ionization source (ESI). All the solvents were of HPLC grade (Fluka). Mass spectral (MS) data were obtained using an Agilent 1100 LC/MSD VL system (G1946C) with a 0.4 mL/min flow rate using a binary solvent system of 95:5 methyl alcohol/water. UV detection was monitored at 254 nm. Mass spectra were acquired in positive mode scanning over the mass range of 50–1500. The following ion source parameters were used: drying gas flow, 9 mL/min; nebulize pressure, 40 psig; and drying gas temperature, 350 °C.

5.2. Parallel synthesis of pyrazolones **7a–k**

Appropriate β -ketoesters, partitioned into 11 different vessels (3 mmol), were placed in the Büchi Syncore[®] and dissolved in EtOH (5 mL). Appropriate phenylhydrazines (3 mmol) were then added. The reaction mixtures were refluxed at 300 rpm for 3 h. To the cooled solutions, *p*-toluenesulfonic acid polymer-bound scavenger was added (0.2 equiv/mol) and the mixtures were stirred (300 rpm) for 2 h at rt. The reaction mixtures were filtered in parallel with a specific filtration unit and the scavengers were washed twice with CH₂Cl₂ (10 mL). The solvents were evaporated to

Table 1



Compound	R	R ₁	MIC (μg/mL) <i>M. tuberculosis</i>
1	Cl	CH ₃	6.25
2	H	CH ₃	6.25
3	F	CH ₃	12.5
8a	H	CF ₃	>64
8b	H	Isopropyl	64
8c	H	Ph	32
8d	Cl	CF ₃	>64
8e	Cl	Isopropyl	32
8f	Cl	Ph	16
8g	Br	CH ₃	4
8h	CH ₃	CH ₃	16
8i	CH ₃	Ph	32
8j	Isopropyl	CH ₃	16
8k	Isopropyl	Ph	32
4	H	CH ₃	>100
9a	H	4-F-Bn	32
9b	H	Bn	>64
9c	H	4-NO ₂ -Bn	>32
9d	Cl	4-F-Bn	32
9e	Cl	Bn	16
9f	Cl	4-NO ₂ -Bn	32

dryness in the same apparatus. Compounds **7a–k** were recrystallized from Et₂O (40–60% yield after crystallization). After crystallization, compounds **7a–k** were identified by LC/MS analysis and proved to be pure enough (>90%) to be used in the next step without further purification.

7a: Yield 40%. ¹H NMR (CDCl₃): δ 7.70–7.33 (5H, m, Ph), 5.90 (1H, s, CH), 3.35 (1H, br s, OH). MS: *m/z* 212 (M⁺).

7b: Yield 48%. ¹H NMR (CD₃OD): δ 7.65–7.26 (5H, m, Ph), 3.34 (2H, s, CH₂), 2.84 (1H, m, CH₃CHCH₃), 1.26 (6H, d, *J* = 6.9 Hz, CH₃CHCH₃). MS: *m/z* 203 (M⁺).

7c: Yield 60%. ¹H NMR (CD₃OD): δ 7.96 (2H, m, Ph), 7.73 (2H, m, Ph), 7.69–7.22 (6H, m, Ph), 3.73 (2H, s, CH₂). MS: *m/z* 237 (M⁺).

7d: Yield 46%. ¹H NMR (CDCl₃): δ 7.73 (2H, d, *J* = 8.8 Hz, Ph), 7.53 (2H, d, *J* = 8.8 Hz, Ph), 5.91 (1H, s, CH), 3.30 (1H, br s, OH). MS: *m/z* 247 (M⁺).

7e: Yield 54%. ¹H NMR (CD₃OD): δ 7.55 (2H, d, *J* = 8.7 Hz, Ph), 7.35 (2H, d, *J* = 8.7 Hz, Ph), 6.08 (1H, s, CH), 3.16 (1H, m, CH₃CHCH₃), 1.29 (6H, d, *J* = 6.9 Hz, CH₃CHCH₃). MS: *m/z* 237 (M⁺).

7f: Yield 60%. ¹H NMR (CDCl₃): δ 7.96–7.72 (4H, m, Ph), 7.50–7.28 (5H, m, Ph), 3.83 (2H, s, CH₂). MS: *m/z* 271 (M⁺).

7g: Yield 52%. ¹H NMR (CDCl₃): δ (ppm) 7.78 (2H, d, *J* = 9.3 Hz, Ph), 7.47 (2H, d, *J* = 9.3 Hz, Ph), 3.41 (2H, s, CCH₂CO), 2.18 (3H, s, CH₃). MS: *m/z* 253–255 (M+1)⁺, 275–277 (M+Na)⁺, 529–531 (2M+Na)⁺.

7h: Yield 60%. ¹H NMR (CDCl₃): δ 7.43 (2H, d, *J* = 8.0 Hz, Ph), 7.17 (2H, d, *J* = 8.0 Hz, Ph), 6.05 (1H, s, CH), 2.35 (3H, s, CH₃), 2.30 (3H, s, CH₃). MS: *m/z* 189 (M⁺).

7i: Yield 59%. ¹H NMR (CDCl₃): δ 7.83 (2H, m, Ph), 7.41–7.05 (7H, m, Ph), 3.81 (2H, s, CH₂), 2.14 (3H, s, CH₃). MS: *m/z* 251 (M⁺).

7j: Yield 52%. ¹H NMR (CD₃OD): δ 7.50–7.25 (5H, m, Ph), 5.59 (1H, s, CH), 2.90 (1H, m, CH₃CHCH₃), 2.19 (3H, s, CH₃), 1.23 (6H, d, *J* = 6.8 Hz, CH₃CHCH₃). MS: *m/z* 217 (M⁺).

7k: Yield 57%. ¹H NMR (CDCl₃): δ 7.83 (2H, m, Ph), 7.44–7.16 (7H, m, Ph), 3.82 (2H, s, CH₂), 2.77 (1H, m, CH₃CHCH₃), 1.10 (6H, d, *J* = 6.8 Hz, CH₃CHCH₃). MS: *m/z* 279 (M⁺).

5.3. Parallel synthesis of pyrazoles 8a–k

Pyrazolones **7a–k**, partitioned into 11 different vessels (1 mmol), were placed in the Büchi Syncore[®] and dissolved in dioxane (10 mL). Ca(OH)₂ (2 equiv/mol) and *p*-chlorobenzoyl chloride (1 equiv/mol) were then added. The reaction mixtures were refluxed at 300 rpm for 3 h. The cooled solutions were evaporated in parallel under vacuum to dryness. HCl (3 N) was added to precipitate crude compounds **8a–k** which were then filtered in parallel and recrystallized from EtOH.

8a: Yield 58%. ¹H NMR ((CD₃)₂SO): δ 7.97–7.84 (m, 4H, Ph), 7.63–7.39 (m, 5H, Ph), 6.96 (br s, 1H, OH). MS: *m/z* 367 (M⁺), 389 (M+Na). Anal. for C₁₇H₁₀ClF₃N₂O₂ Calcd%: C, 55.68; H, 2.75; N, 7.64. Found%: C, 55.79; H, 2.89; N, 7.89.^{9b}

8b: Yield 54%. ¹H NMR ((CD₃)₂SO): δ 7.68–7.66 (m, 4H, Ph), 7.58–7.23 (m, 5H, Ph), 3.35 (1H, m, CH₃CHCH₃), 1.12 (6H, d, *J* = 6.8 Hz, CH₃CHCH₃). MS: *m/z* 342 (M⁺), 364 (M+Na). Anal. for C₁₉H₁₇ClN₂O₂ Calcd%: C, 66.96; H, 5.03; N, 8.22. Found%: C, 67.07; H, 5.23; N, 8.45.

8c: Yield 70%. ¹H NMR ((CD₃)₂SO): δ 7.74–7.16 (m, 14H, Ph). MS: *m/z* 375 (M⁺), 397 (M+Na). Anal. for C₂₂H₁₅ClN₂O₂ Calcd%: C, 70.50; H, 4.03; N, 7.47. Found%: C, 70.69; H, 4.22; N, 7.65.

8d: Yield 61%. ¹H NMR ((CD₃)₂SO): δ 7.98–7.84 (m, 4H, Ph), 7.68–7.47 (m, 4H, Ph), 6.94 (br s, 1H, OH). MS: *m/z* 402 (M⁺), 424 (M+Na). Anal. for C₁₇H₉Cl₂F₃N₂O₂ Calcd%: C, 50.90; H, 2.26; N, 6.98. Found%: C, 50.99; H, 2.45; N, 6.89.^{9b}

8e: Yield 63%. ¹H NMR ((CD₃)₂SO): δ 7.75–7.69 (m, 4H, Ph), 7.51–7.46 (m, 4H, Ph), 3.22 (1H, m, CH₃CHCH₃), 1.17 (6H, d, *J* = 6.9 Hz, CH₃CHCH₃). MS: *m/z* 376 (M⁺), 398 (M+Na). Anal. for C₁₉H₁₆Cl₂N₂O₂ Calcd%: C, 60.81; H, 4.30; N, 7.47. Found%: C, 60.99; H, 4.56; N, 7.59.

8f: Yield 69%. ¹H NMR ((CD₃)₂SO): δ 7.88–7.52 (m, 6H, Ph), 7.36–7.21 (m, 7H, Ph). MS: *m/z* 410 (M⁺), 432 (M+Na). Anal. for C₂₂H₁₄Cl₂N₂O₂ Calcd%: C, 64.56; H, 3.45; N, 6.84. Found%: C, 64.67; H, 3.67; N, 6.90.

8g: Yield 35%. ¹H NMR (CDCl₃): δ (ppm) 7.81–7.75 (2H, m, Ph), 7.60–7.46 (6H, m, Ph), 2.09 (3H, s, CH₃). MS: *m/z* 389–391 (M–1)⁺. Anal. for C₁₇H₁₂BrClN₂O₂ Calcd%: C, 52.13; H, 3.09; N, 7.15. Found%: C, 52.23; H, 3.10; N, 7.16.

8h: Yield 68%. ¹H NMR (CDCl₃): δ 7.70 (d, 2H, *J* = 8.5 Hz, Ph), 7.58 (d, 2H, *J* = 8.6 Hz, Ph), 7.47 (d, 2H, *J* = 8.6 Hz, Ph), 7.25 (d, 2H, *J* = 8.5 Hz, Ph), 2.37 (s, 3H, CH₃), 2.09 (s, 3H, CH₃). MS: *m/z* 327 (M⁺), 349 (M+Na). Anal. for C₁₈H₁₅ClN₂O₂ Calcd%: C, 66.16; H, 4.63; N, 8.57. Found%: C, 66.34; H, 4.87; N, 8.76.

8i: Yield 68%. ¹H NMR ((CD₃)₂SO): δ 7.68–7.59 (m, 4H, Ph), 7.34–7.20 (m, 9H, Ph), 2.33 (s, 3H, CH₃). MS: *m/z* 389 (M⁺), 411 (M+Na). Anal. for C₂₃H₁₇ClN₂O₂ Calcd%: C, 71.04; H, 4.41; N, 7.20. Found%: C, 71.34; H, 4.65; N, 7.34.

8j: Yield 61%. ¹H NMR ((CD₃)₂SO): δ 7.67–7.65 (m, 2H, Ph), 7.49–7.45 (m, 4H, Ph), 7.28–7.26 (m, 2H, Ph), 2.84 (1H, m, CH₃CHCH₃), 2.18 (s, 3H, CH₃), 1.13 (6H, d, *J* = 6.7 Hz, CH₃CHCH₃). MS: *m/z* 355 (M⁺), 377 (M+Na). Anal. for C₂₀H₁₉ClN₂O₂ Calcd%: C, 67.70; H, 5.40; N, 7.89. Found%: C, 67.89; H, 5.67; N, 7.94.

8k: Yield 70%. ¹H NMR ((CD₃)₂SO): δ 7.77–7.59 (m, 4H, Ph), 7.38–7.21 (m, 9H, Ph), 2.93 (1H, m, CH₃CHCH₃), 1.21 (6H, d, *J* = 6.8 Hz, CH₃CHCH₃). MS: *m/z* 417 (M⁺), 439 (M+Na). Anal. for C₂₅H₂₁ClN₂O₂ Calcd%: C, 72.02; H, 5.08; N, 6.72. Found%: C, 72.34; H, 5.23; N, 6.87.

5.4. Parallel synthesis of pyrazoles 9a–f

Compounds **1** and **2** (0.5 mmol),⁴ divided into six different vessels, were placed in the Büchi Syncore® and dissolved in dry DMF (5 mL). NaH (2 equiv/mol) was added and the reaction mixtures were stirred at 300 rpm for 1 h. The appropriate benzyl chloride (or benzyl bromide) (1 equiv/mol) and NaI (cat.) were then added and the resulting mixtures were stirred at rt at 300 rpm overnight. Water (5 mL) and AcOEt (5 mL) were added and the resulting mixtures were stirred for 1 h. The organic layers were then filtered out in parallel and evaporated to dryness to afford crude compounds **9a–f**, which were purified by flash chromatography (hexanes/ethyl acetate 4:1) to afford the final products (20–73% yield).

9a: Yield: 50%. ¹H NMR (CDCl₃): δ (ppm) 7.73 (2H, d, *J* = 8.13 Hz, Ph), 7.38–7.28 (5H, m, Ph), 6.90 (2H, d, *J* = 7.71 Hz, Ph), 6.83–6.81 (2H, m, Ph), 6.81–6.79 (2H, m, Ph), 4.82 (2H, s, NCH₂Ph), 2.57 (3H, s, CH₃). MS: *m/z* 421–423 (M+1)⁺; 443–445 (M+Na)⁺; 863 (2M+Na)⁺. Anal. for C₂₄H₁₈ClFN₂O₂ Calcd%: C, 68.49; H, 4.31; N, 6.66. Found%: C, 68.63; H, 4.32; N, 6.67.

9b: Yield: 20%. ¹H NMR (CDCl₃): δ (ppm) 7.76 (2H, d, *J* = 8.33 Hz, Ph), 7.39–7.715 (10H, m, Ph), 6.88–6.86 (2H, m, Ph), 4.88 (2H, s, NCH₂Ph), 2.61 (3H, s, CH₃). MS: *m/z* 403–405 (M+1)⁺; 425–427 (M+Na)⁺; 827–829 (2M+Na)⁺. Anal. for C₂₄H₁₉ClN₂O₂ Calcd%: C, 71.55; H, 4.75; N, 6.95. Found%: C, 71.76; H, 4.76; N, 6.97.

9c: Yield: 60%. ¹H NMR (CDCl₃): δ (ppm) 8.09 (2H, d, *J* = 8.61 Hz, Ph), 7.75 (2H, d, *J* = 8.52 Hz, Ph), 7.37–7.28 (5H, m, Ph), 7.13 (2H, d, *J* = 7.7 Hz, Ph), 7.02 (2H, d, *J* = 8.61 Hz, Ph), 4.94 (2H, s, NCH₂Ph), 2.58 (3H, s, CH₃). MS: *m/z* 448–450 (M+1)⁺; 470–472 (M+Na)⁺; 486 (M+K)⁺; 917–919–918 (2M+Na)⁺. Anal. for C₂₄H₁₈ClN₃O₄ Calcd%: C, 64.36; H, 4.05; N, 9.38. Found%: C, 64.62; H, 4.06; N, 9.42.

9d: Yield: 73%. ¹H NMR (CDCl₃): δ (ppm) 7.75 (2H, d, *J* = 8.28 Hz, Ph), 7.37–6.80 (10H, m, Ph), 4.82 (2H, s, NCH₂Ph), 2.60 (3H, s, CH₃). MS: *m/z* 455–457 (M+1)⁺; 477–479 (M+Na)⁺; 933–931 (2M+Na)⁺. Anal. for C₂₄H₁₇Cl₂FN₂O₂ Calcd%: C, 63.31; H, 3.76; N, 6.15. Found%: C, 63.76; H, 3.77; N, 6.16.

9e: Yield: 20%. ¹H NMR (CDCl₃): δ (ppm) 7.78 (2H, d, *J* = 8.00 Hz, Ph), 7.41–7.13 (9H, m, Ph), 6.92–6.90 (2H, m, Ph), 4.91 (2H, s, NCH₂Ph), 2.66 (3H, s, CH₃). MS: *m/z* 437–439 (M+1)⁺; 459–461 (M+Na)⁺; 895–897 (2M+Na)⁺. Anal. for C₂₄H₁₈Cl₂N₂O₂ Calcd%: C, 65.91; H, 4.15; N, 6.41. Found%: C, 66.04; H, 4.16; N, 6.42.

9f: Yield: 30%. ¹H NMR (CDCl₃): δ (ppm) 8.13 (2H, d, *J* = 8.75 Hz, Ph), 7.77 (2H, d, *J* = 7.99 Hz, Ph), 7.40–7.31 (4H, m, Ph), 7.15–7.06 (4H, m, Ph), 4.97 (2H, s, NCH₂Ph), 2.61 (3H, s, CH₃). MS: *m/z* 504–506 (M+Na)⁺; 987 (2M+Na)⁺. Anal. for C₂₄H₁₇Cl₂N₃O₄ Calcd%: C, 59.77; H, 3.55; N, 8.71. Found%: C, 59.95; H, 3.56; N, 8.73.

6. Microbiological assays

6.1. Mycobacterial strain

M. tuberculosis H37Rv ATCC 27294 was used in this study. It was maintained on Löwenstein-Jensen (bioMérieux, Marcy l'Étoile, France) agar slants until needed.

6.2. Antimicrobial susceptibility testing

MICs were determined by a standard twofold agar dilution method. Briefly, 1 mL of Middlebrook 7H11 agar (Becton Dickinson BBL, Sparks, MD) supplemented with 10% oleic acid-albumin-dextrose-catalase enrichment containing the testing compounds in 24-multiwell plates at concentrations ranging between 0.0312 and 64 µg/mL was inoculated with 10 µL of a suspension containing *M. tuberculosis* H37Rv 1.5×10^5 cfu/mL grown on Middlebrook 7H9 broth (Difco Laboratories, Detroit, MI) supplemented with 10% albumin-dex-

trose-catalase enrichment. Final inoculum was 1.5×10^3 per well and was obtained as described previously.¹⁴ Plates were incubated for 21–28 days and MICs were read as minimal concentrations of compounds completely inhibiting visible growth of mycobacteria.

7. Computational details

Computational analysis was performed by means of the Catalyst software package, version 4.10.¹⁰

All the compounds were built using the 2D/3D sketcher of the program. A representative family of conformations was generated for each molecule using the CHARMM force field implemented in Catalyst, together with the Poling algorithm and the best quality conformational analysis method.^{15,16} Conformational diversity was emphasized by selection of the conformers that fell within a 20 kcal/mol range above the lowest-energy conformation. The Compare/Fit command in the Hypothesis Generation workbench was used to analyze the mapping mode of compounds within the pharmacophoric model. In particular, the Best Fit option was applied, which manipulates conformers within the specified energy threshold to minimize the distances between hypothesis features and mapped atoms in the molecule.

Acknowledgments

Financial support from the Italian Ministero dell'Istruzione, dell'Università e della Ricerca (PRIN 2005037820) is gratefully acknowledged. CARIPO (Grant Rif. 2006.0880/10.8485 Bando 2006) is gratefully acknowledged. We thank Asinex for partial financial support for this work.

References and notes

- (a) World Health Organization: The World Health Organization Global Tuberculosis Program, 2007. <http://www.who.int/gtb>; http://www.who.int/tb/publications/global_report/2007/pdf/full; (b) Espinal, M. A. *Tuberculosis* **2003**, 83, 44; (c) Frieden, T. R.; Munsiff, S. S. *Clin. Chest Med.* **2005**, 26, 197; (d) Burman, W. J. *Clin. Chest Med.* **2005**, 26, 283.
- World Health Organization, TB Home, 2007. <http://www.who.int/tb/en/>.
- (a) Janin, Y. L. *Bioorg. Med. Chem.* **2007**, 15, 2479; (b) O'Brien, R. J.; Nunn, P. P. *Am. J. Respir. Crit. Care Med.* **2001**, 1635, 1055; (c) Ahmad, Z.; Pandey, R.; Sharma, S.; Khuller, G. K. *Int. J. Antimicrob. Agents* **2008**, 31, 142.
- Manetti, F.; Magnani, M.; Castagnolo, D.; Passalacqua, L.; Botta, M.; Corelli, F.; Saggi, M.; Deidda, D.; De Logu, A. *ChemMedChem* **2006**, 1, 973.
- Kutterer, K. M.; Davis, J. M.; Singh, G.; Yang, Y.; Hu, W.; Severin, A.; Rasmussen, B. A.; Krishnamurthy, G.; Failli, A.; Katz, A. H. *Bioorg. Med. Chem. Lett.* **2005**, 15, 2527.
- Pyrazolones **7a–k** can exist in three tautomeric forms as indicated in Scheme 1. ¹H NMR analysis revealed the presence of a single signal set due to the quick chemical exchange between the three tautomeric forms.
- Jensen, B. S. *Acta Chem. Scand.* **1959**, 13, 1668.
- Holzer, W.; Kautsch, C.; Laggner, C.; Claramunt, R. M.; Pérez-Torrallba, M.; Alkorta, I.; Elguero, J. *Tetrahedron* **2004**, 60, 6791.
- (a) Holzer, W.; Hahn, K.; Brehmer, T.; Claramunt, R. M.; Pérez-Torrallba, M. *Eur. J. Org. Chem.* **2003**, 7, 1209; (b) Bieringer, S.; Holzer, W. *Heterocycles* **2006**, 68, 1825.
- NOE interactions between benzyl protons and methyl at C3 was revealed, whereas no NOE interactions between benzyl and *p*-chlorophenyl protons were observed.
- Catalyst, version 4.10, Accelrys Inc., San Diego, CA. <http://www.accelrys.com>.
- Manetti, F.; Corelli, F.; Biava, M.; Fioravanti, R.; Porretta, G. C.; Botta, M. *Farmaco* **2000**, 55, 484.
- The weaker activity of fluoro-derivative **3** seems to be in contrast with pharmacophoric investigations and biological data of the other N1-*p*-halogen compounds. However, we hypothesized that the electron-withdrawing fluorine atom might have an inductive effect on the pyrazole nucleus and alteration of its electronic nature might resolve into a loss of activity.
- De Logu, A.; Onnis, V.; Saggi, B.; Congiu, C.; Schivo, M. L.; Cocco, M. T. *J. Antimicrob. Chemother.* **2002**, 49, 275.
- Brooks, B. R.; Brucoleri, R. E.; Olafson, B. D.; States, D. J.; Swaminathan, S.; Karplus, M. *J. Comput. Chem.* **1983**, 4, 187.
- (a) Smellie, A.; Teig, S. L.; Towbin, P. J. *Comput. Chem.* **1995**, 16, 171; (b) Smellie, A.; Kahn, S. D.; Teig, S. L. *J. Chem. Inf. Comput. Sci.* **1995**, 35, 285; (c) Smellie, A.; Kahn, S. D.; Teig, S. L. *J. Chem. Inf. Comput. Sci.* **1995**, 35, 295.